Fluctuation-induced first-order transitions and symmetry-breaking fields: The $n=3$-component cubic model

Daniel Blankschtein
Department of Physics and Astronomy, Tel-Aviv University, Ramat Aviv, Israel

David Mukamel*
IBM Thomas J. Watson Research Center, Yorktown Heights, New York 10598
(Received 7 July 1981)

The effects of an off-diagonal quadratic symmetry-breaking field, g, on a three-component ($n=3$) cubic model with no accessible fixed points are studied. It is shown that this perturbation induces a crossover from first-order to continuous transition. Depending upon the initial values of the parameters characterizing the model, two types of (g,T) phase diagrams are possible, both of which are rather complex, exhibiting tricritical, critical, and critical end points. The (g,T) phase diagrams are studied using large-g expansion, mean-field theory, and renormalization-group analysis. A universal amplitude ratio associated with the critical end points is calculated to leading (zeroth) order in $\epsilon=4-d$. The phase diagrams are predicted to be realizable in certain $n=3$ cubic crystals undergoing structural phase transitions, such as $BaTiO_3$, $RbCaF_3$, and $KMnF_3$.

I. INTRODUCTION

Phase transitions which are continuous within mean-field approximation, but which are driven first order by critical fluctuations have been a subject of considerable interest in recent years.[1–15] Within the renormalization-group approach this may occur either when the appropriate model does not possess a stable fixed point[1–7] or when the stable fixed point is not physically accessible.[8–10] In these cases the initial Hamiltonian does not flow to a fixed-point Hamiltonian under the renormalization-group transformation, but rather to a region in its parameter space where it becomes thermodynamically unstable (i.e., the fourth-order terms are no longer positive definite). A direct integration of the renormalization-group recursion relations, to yield the free energy, then shows that under such circumstances the transition becomes first order.[8–10] By applying a symmetry-breaking field, g, a fixed point which is both stable and accessible may emerge and the transition may become second order. The crossover from first-order to continuous transition induced by symmetry-breaking fields has been studied quite extensively in recent years.[11,12,14–16] Domany, Mukamel, and Fisher[12] have applied large-g expansions, renormalization-group techniques, and mean-field calculation to study the (g,T) phase diagram of a relatively simple n-component Landau-Ginzburg-Wilson (LGW) Hamiltonian with cubic anisotropy, for which the stable fixed point is inaccessible. The symmetry-breaking field, g, corresponds to uniaxial anisotropy along a principal direction. This study has been extended[15,16] to consider the most general symmetry-breaking field for the particular case in which the number of components of the order parameter is $n=2$. Subsequently,[16] the phase diagrams of more complicated models which do not possess a stable fixed point have been analyzed. It has been found that these phase diagrams are rather complex, exhibiting tricritical, fourth-order critical and critical end points. Experimentally, the crossover from first-order to continuous transition has been observed in MnO (Refs. 17,18) under a [111] uniaxial stress, and more recently in $RbCaF_3$ [Refs. 19(a) and 19(b)] under a [100] uniaxial stress.

In the present paper, we consider the $n=3$ component cubic model and study its (g,T) phase diagram, where g corresponds to a uniaxial stress along a body diagonal. The LGW model takes the form

$$H=\int d^dx\,\mathcal{H}\ , \tag{1.1a}$$

where

$$\mathcal{H}=-\frac{1}{2}r\sum_{i=1}^{3}S_i^2-\frac{1}{2}\sum_{i=1}^{3}(\nabla S_i)^2 - u\sum_{i=1}^{3}S_i^4-v\sum_{i<j=1}^{3}S_i^2S_j^2\ . \tag{1.1b}$$

For stability of the free energy we require

$$u>0 \text{ and } u+v>0\ . \tag{1.2}$$

The partition function is given by $Z=\mathrm{tr}e^{\mathcal{H}}$. Renormalization-group studies[20,21] indicate that in $d=3$ dimensions the model possesses an isotropic

($v^*=2u^*$) stable fixed point. Within the ϵ expansion this model is found to have two regions in the (u,v) plane (with u and v of order ϵ) which lie outside the domain of attraction of the stable fixed point[21]

$$w=v-3u+O(\epsilon^2)>0 \ , \tag{1.3a}$$

and

$$v<0 \ , \tag{1.3b}$$

(see Fig. 1). If one starts with a Hamiltonian whose parameters are in regions (a) or (b), one encounters a "runaway" and the transition becomes first order.[8–10] This result is to be contrasted with the mean-field prediction of a continuous phase transition for all values of (u,v) inside the stability wedge, (1.2). We consider the (g,T) phase diagram associated with the model (1.1) in region (1.3a) ($w>0$), and in region (1.3b) ($v<0$), where g is a quadratic symmetry-breaking field which enters into the Hamiltonian (1.1b) via the term

$$g(S_1S_2+S_2S_3+S_3S_1) \ . \tag{1.4}$$

Previous studies were restricted to symmetry-breaking fields which enter into the Hamiltonian via terms of the form[12] $g_1[(S_1^2+S_2^2)-2S_3^2]$ and $g_2(S_1^2-S_2^2)$.[16] The easy axis associated with $g>0$ lies along the [111] direction in the (S_1,S_2,S_3) space, while for $g<0$ the easy axes lie in the (111) plane. For $v-2u>0$, the quartic terms favor the [100], [010], and [001] axes, whereas when $v-2u<0$ they favor the [111], $[\bar{1}11]$, $[1\bar{1}1]$, and $[11\bar{1}]$ axes. The (g,T) phase diagrams for both $v-2u>0$ and $v-2u<0$, associated with an accessible isotropic fixed point, have been studied extensively both theoretically and experimentally in recent years.[22,23] When $v-2u<0$ and $g=0$ the model predicts a second-order transition at $T=T_B(g=0)$ in which the system orders along one of the cube diagonals.[22] For $g>0$ there is no competition since both g and the quartic term prefer the [111] direction, hence the second-order phase transition is predicted to occur at $T_c(g)$ (line α of Fig. 2a). A large and negative g prefers ordering in the (111) plane. Therefore it is obvious that as one lowers $|g|(g<0)$ the order parameter will rotate towards one of the directions $[\bar{1}11]$, $[1\bar{1}1]$, or $[11\bar{1}]$ but not towards [111]. We thus expect the line $g=0$, $T<T_B$ to be a first-order line above which ordering occurs in the [111] direction and below which there is an intermediate phase in which ordering occurs along $[\alpha\alpha\beta]$ [when $g=0$

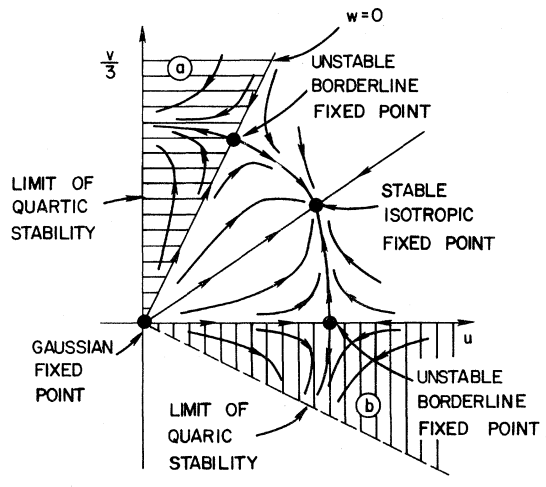

FIG. 1. Schematic renormalization-group flow diagram in the (u,v) plane for the $n=3$ cubic model. The stable isotropic (Heisenberg) fixed point is not accessible from the two shaded regions (a) $w>0$ and (b) $v<0$. The stability limits $u=0$, $v>0$ and $u+v=0$, $u>0$ are shown.

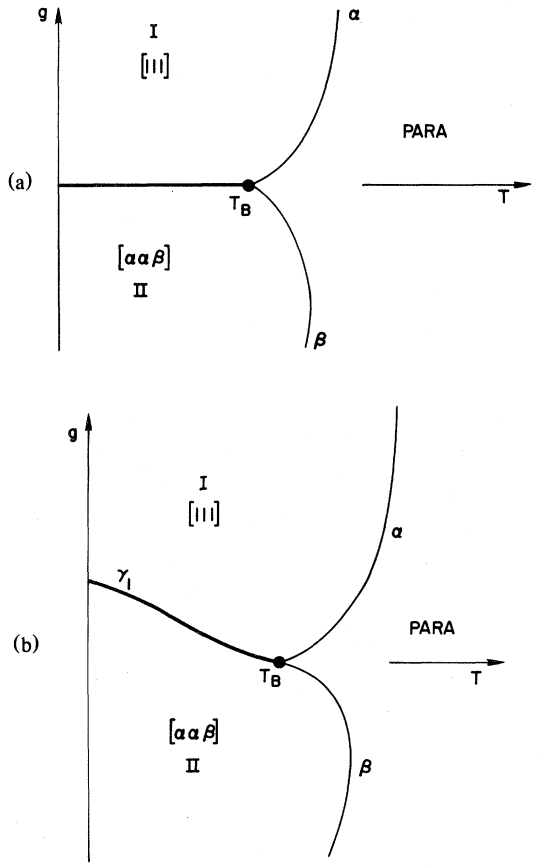

FIG. 2. (a) Schematic (g,T) phase diagram associated with the $n=3$ cubic model with easy axes along the cube diagonals ($v-2u<0$) when the stable isotropic fixed point is accessible. Thin lines represent continuous transitions, thick lines represent first-order transitions. The direction of the order parameter $\vec{S}$ in the two ordered phases I and II is indicated. The point $T=T_B$, $g=0$ is bicritical. (b) Same as Fig. 2(a) but with easy axes along the cube edges ($v-2u>0$).

one has ($\alpha=1$, $\beta=-1$)]. The transition from the disordered phase into the intermediate phase is also second order [line β of Fig. 2(a)]. The point $T=T_B$, $g=0$ is therefore bicritical[22] [see Fig. 2(a)]. When $v-2u>0$ and $g=0$ the model predicts a second-order transition at $T=T_B$ in which the system orders along one of the cube axes. For $g>0$ the quartic and quadratic anisotropies compete. For large g, the system exhibits a second-order transition associated with [111] ordering.[23] As g is lowered, there is a second phase transition, at which the components of $\vec{S}$ in the (111) plane order as well. This is a $q=3$-state Potts transition line[23,24] [line γ_1 of Fig. 2(b)]. Renormalization-group studies in $d=4-\epsilon$ dimensions predicted that this transition should be first order. For a negative g the transition from the disordered phase into the intermediate phase is second order and no additional transition occurs[23] [see Fig. 2(b)]. These predictions were first checked and confirmed in $SrTiO_3$ stressed along the [111] direction.[23]

In this paper we show that when the isotropic fixed point is not accessible, namely either $w>0$ or $v<0$, the (g,T) phase diagrams of Figs. 2(a) and 2(b) change dramatically. For the case $v-2u<0$, one obtains a phase diagram displaying two critical lines, a line of first-order transitions which terminates at a critical point, a critical end point, and a tricritical point [see Fig. 3(a)]. For the case $v-2u>0$, the phase diagram displays two critical lines, a line of first-order transitions terminating at a critical point, and two critical end points [see Fig. 3(b)]. The phase diagrams have been studied in the limit of large symmetry-breaking field ($g>>1$) using perturbation expansion in u and v. In order to substantiate these results we have performed a mean-field analysis of the problem. To describe a first-order transition within the context of mean-field theory, it is necessary to assume that the quartic terms are not positive definite, which implies that one should add a sixth-order term to the otherwise thermodynamically unstable Hamiltonian. The qualitative features of the phase diagrams are found to be the same in both methods. We have then studied the limit of very small symmetry-breaking field $|g|<<1$ using renormalization-group methods in $d=4-\epsilon$ dimensions. The existence of tricritical and critical- end points was confirmed and a universal amplitude ratio between the parameters characterizing the critical end points was calculated to leading (zeroth) order in ϵ.

In outline, the remainder of the paper is as follows: In Sec. II we analyze the phase diagram of the $n=3$ cubic model lying in region (1.3a), $w>0$ in the limit of large g. The mean-field approximation is considered in Sec. III. In Sec. IV we analyze the $n=3$ cubic model lying in region (1.3b), $v<0$. The calculations are performed both in the large-g limit and the mean-field approximation. Most of the calculations are similar to those in Secs. II and III and therefore we merely quote results. In Sec. V we discuss the limit $|g|<<1$ using renormalization-group techniques in $d=4-\epsilon$ dimensions. Using scaling arguments we obtain a definition of a universal amplitude ratio associated with the critical end points and we calculate this ratio to leading (zeroth) order in ϵ. Sec. VI contains our conclusions.

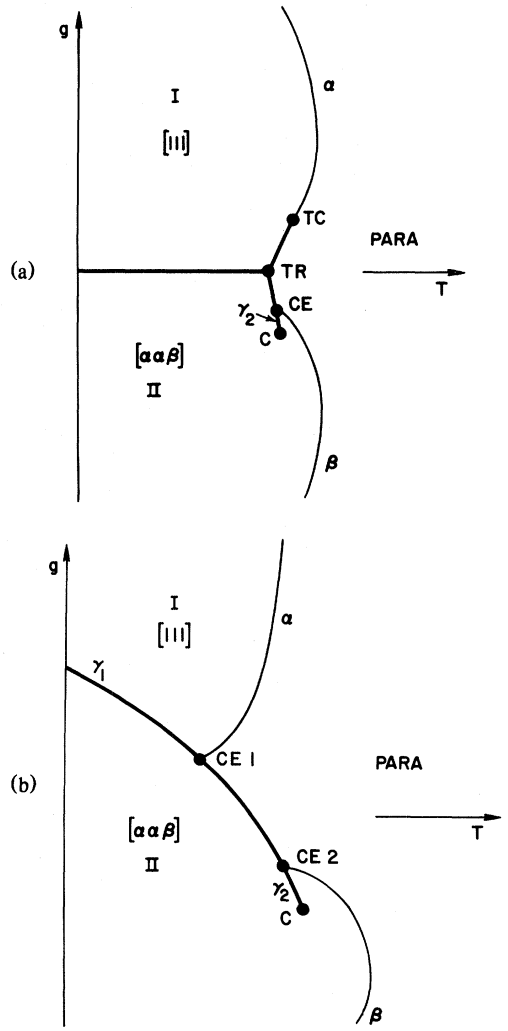

FIG. 3. (a) Schematic (g,T) phase diagram associated with the $n=3$ cubic model with easy axes along the cube diagonals ($v-2u<0$) when the stable isotropic fixed point is not accessible ($-u<v<0$) [region (b) of Fig. 1]. Thin lines represent continuous transitions and thick lines represent first-order transitions. The point TC is tricritical, C is a critical point and CE a critical end point and TR is a triple point. (b) Schematic (g,T) phase diagram associated with the $n=3$ cubic model with easy axes along the cube edges ($v-2u>0$) when the stable isotropic fixed point is not accessible ($0<u<v/3$) [region (a) of Fig. 1]. The points CE1 and CE2 are critical end points, C is a critical point.

II. CUBIC MODEL WITH $w > 0$: LARGE-g LIMIT

Consider the $n=3$ cubic Hamiltonian (1.1). We assume that the Hamiltonian lies in region (a) of Fig. 1, namely, it is outside the domain of attraction of the isotropic fixed point, but within the stability wedge. This Hamiltonian exhibits a first-order transition.[8,9] Consider now an anisotropy field, g, which introduces a coupling term

$$g(S_1S_2+S_2S_3+S_3S_1) \ , \tag{2.1}$$

into the Hamiltonian. It is convenient to rotate the coordinates, so that one component is along [111] and the other two are in the plane perpendicular to [111], namely, the (111) plane. This rotation ensures the diagonalization of the quadratic terms in the Hamiltonian. To be specific, we choose[22]

$$\phi_1=\frac{1}{\sqrt{3}}(S_1+S_2+S_3) \ , \tag{2.2}$$

$$\phi_2=\frac{1}{\sqrt{2}}(S_1-S_2) \ , \tag{2.3}$$

$$\phi_3=\frac{1}{\sqrt{6}}(S_1+S_2-2S_3) \ . \tag{2.4}$$

The Hamiltonian now takes the form

$$\begin{aligned}\mathcal{H}=&-\tfrac{1}{2}r_1\phi_1^2-\tfrac{1}{2}r_2|\vec{\phi}_\perp|^2-\tfrac{1}{2}[(\nabla\phi_1)^2+(\nabla\vec{\phi}_\perp)^2]\\&-\tfrac{1}{3}(u+v)\phi_1^4-\tfrac{1}{4}(2u+v)|\vec{\phi}_\perp|^4-2u\phi_1^2|\vec{\phi}_\perp|^2\\&-\tilde{u}\phi_1(\phi_3^3-3\phi_3\phi_2^2) \ ,\end{aligned} \tag{2.5}$$

where

$$\vec{\phi}_\perp^2=\phi_2^2+\phi_3^2, \quad \tilde{u}=-\tfrac{2}{3}\sqrt{2}(u-\tfrac{1}{2}v) \ ,$$

$$r_1=r-\tfrac{2}{3}g, \quad r_2=r+\tfrac{1}{3}g \ .$$

The gross features of the (r,g) phase diagram can be found quite easily. At $g=0$ and low temperatures the system orders along one of the cubic axes [in terms of ϕ_i this means that $\langle\phi_i\rangle\neq 0$, $i=1,2,3$, see Eqs. (2.2)–(2.4)]. The transition to this ordered phase is first order. For large and positive g, the components ϕ_2 and ϕ_3 are suppressed ($r_2 >> r_1$) and the system will order in a phase characterized by $\langle\phi_1\rangle\neq 0$, $\langle\phi_2\rangle=\langle\phi_3\rangle=0$, namely, the order parameter will point along [111]. This phase transition [line α of Fig. 3(b)] is expected to be second order (Ising type with $(u+v)/3>0$). As one lowers g ($g>0$), competition between g and the quartic terms increases, resulting in an additional phase transition in which ϕ_2 and ϕ_3 order as well. From the arguments presented in the Introduction we expect that this transition is first order $q=3$-state Potts-like. For large and negative g, ϕ_1 is suppressed ($r_1 >> r_2$) and the system will order via a second-order xy-like transition [line β of Fig. 3(b)]. Notice that immediately below the transition the component ϕ_1 will also order due to the coupling term $\phi_1(\phi_3^3-3\phi_3\phi_2^2)$. In the (ϕ_2,ϕ_3) subspace there are three preferred directions dictated by the Potts-like term[23] $(\phi_3^3-3\phi_3\phi_2^2)$. These are ($\langle\phi_3\rangle\neq 0$, $\langle\phi_2\rangle=0$, and $\langle\phi_3\rangle/\langle\phi_2\rangle=\pm\sqrt{3}/3$). It will be shown later that the critical lines α and β do not terminate in tricritical points, but rather, in two critical end points CE1 and CE2. A schematic phase diagram which exhibits these features is given in Fig. 3(b). Here we find a first-order transition line inside the ordered phase for $g<0$. This line terminates in a liquid-gas-like critical point C.

In order to establish this picture, we first demonstrate that the two critical lines α and β do not possess tricritical points at large g. In Sec. III we perform a mean-field calculation which shows that these critical lines terminate in critical end points (see Refs. 15 and 16). We then locate the liquid-gas-like critical point C in the large-g limit. Consider the limit of large symmetry-breaking field $|g|\gtrsim 1$, $g>0$, and $u,v<<1$. Furthermore, assume that the Hamiltonian, although stable, is very close to the instability limit, namely, $0<u<<O(v)$. Note that the nature of the phase diagram to be obtained should apply throughout the region (1.3a) since, as is clear from Fig. 1, the renormalization-group flows in this region drive u and v towards the instability limit $u=0$. Near the critical line α, i.e., for $r_1\simeq O(u,v)$, one has $r_2=O(1)$, and the components ϕ_2 and ϕ_3 may be integrated out using perturbation expansion in powers of u and v. One then obtains a reduced Ising-like Hamiltonian

$$\mathcal{H}_{\rm eff}=-\tfrac{1}{2}r_{\rm eff}\phi_1^2-\tfrac{1}{2}(\nabla\phi_1)^2-u_{\rm eff}\phi_1^4-u_6\phi_1^6 \ , \tag{2.6}$$

where to leading order in u and v we find

$$r_{\rm eff}=r_1+8uA_1(r_2,d)+O(u^2,v^2) \ , \tag{2.7}$$

$$u_{\rm eff}=\tfrac{1}{3}(u+v)-8u^2A_2(r_2,d)+O(u^3,v^3) \ , \tag{2.8}$$

while u_6 is of order $O(u^3,v^3)$, and remains positive in the region of interest. The functions $A_n(x,d)$, are given by

$$A_n(x,d)=\int_{|q|\leq 1}\frac{d^dq}{(2\pi)^d}\frac{1}{(x+q^2)^n} \ , \tag{2.9}$$

and d is the spatial dimensionality. Now, in three or more dimensions, the reduced Hamiltonian (2.6) will yield a continuous transition for $r_1\simeq O(u,v)$, $u_{\rm eff}>0$, a first-order transition for $u_{\rm eff}\lesssim 0 (u_6>0)$, and a tricritical point at $r_{\rm eff}\simeq O(u_6)\simeq O(u^3,v^3)$ and $u_{\rm eff}=O(u_6)\simeq O(u^3,v^3)$. In this case however, since for $r_2\gtrsim O(1)$ the integral $A_2(r_2,d)$ satisfies $A_2(r_2,d)\lesssim O(1)$ and $0<u<\frac{1}{3}v$, one finds $u_{\rm eff}>0$ for all positive values of $g\gtrsim 1$, and no tricritical point is found on the critical line α at large g. It is,

in principle, possible that this critical line terminates in a tricritical point located at small g. However, mean-field analysis, which we present in Sec. III, seems to indicate that the critical line α terminates in a *critical end point* [point CE1 of Fig. 3(b)] rather than a tricritical point. Similar arguments may be applied to the critical line β ($g<0$). Near this line one has $r_2 \simeq O(u,v)$ and $r_1 = O(1)$, and the ϕ_1 component of the order parameter may be integrated out. One obtains a reduced xy-like Hamiltonian

$$\mathcal{H}_{\rm eff} = -\tfrac{1}{2} r_{\rm eff} |\vec{\phi}_\perp|^2 - \tfrac{1}{2}(\nabla \vec{\phi}_\perp)^2 - u_{\rm eff} |\vec{\phi}_\perp|^4 - u_6 |\vec{\phi}_\perp|^6 \ , \tag{2.10}$$

where to leading order in u and v we find

$$r_{\rm eff} = r_2 + 4uA_1(r_1,d) + O(u^2,v^2) \ , \tag{2.11}$$

$$u_{\rm eff} = \tfrac{1}{4}(2u+v) - 4u^2 A_2(r_1,d) + O(u^3,v^3) \ , \tag{2.12}$$

and $u_6 \approx O(u^3,v^3)$ is positive in the region of interest. Again for $0<u<<O(v)$ one has $u_{\rm eff}>0$, and no tricritical point is found on the critical line β [defined by $r_{\rm eff} \approx O(u,v)$]. This critical line is expected to terminate in a critical end point [point CE2 of Fig. 3(b)]. The two ordered phases (I) $\langle \phi_1 \rangle \neq 0$, $\langle \vec{\phi}_\perp \rangle = 0$ and (II) $\langle \phi_1 \rangle$, $\langle \vec{\phi}_\perp \rangle \neq 0$ are separated by a transition line γ_1 [see Fig. 3(b)]. The order parameter associated with this transition is $\vec{\phi}_\perp$, and the LGW model has a $q=3$-state Potts-like symmetry (for details see Refs. 24 and 23). This transition is expected to be first order in $d=3$ dimensions. To conclude our analysis we locate the liquid-gas-like critical point C. The calculation is rather tedious and we outline it briefly. Consider the Hamiltonian (2.5) with $r_2 < r_1$ (i.e., $g<0$). In the ordered phase II one has $\langle \phi_1 \rangle = M_1$, $\langle \phi_3 \rangle = M_3$, and $\langle \phi_2 \rangle = 0$. We therefore define a shift in the order parameter

$$\phi_i = M_i + \eta_i, \quad i=1,2,3 \ , \tag{2.13}$$

where $M_2=0$ and M_1 and M_3 are determined by the equations

$$r_1 M_1 + \tfrac{4}{3}(u+v)M_1^3 + 4uM_1 M_3^2 - \frac{\sqrt{2}}{3}(2u-v)M_3^3 = 0 \ , \tag{2.14}$$

$$r_2 M_3 + (2u+v)M_3^3 + 4uM_1^2 M_3 - \sqrt{2}(2u-v)M_1 M_3^2 = 0 \ . \tag{2.15}$$

The Hamiltonian (2.5) now takes the form

$$\mathcal{H} = \mathcal{H}(M_1,M_3) - \frac{1}{2}\sum_{i=1}^{3} \bar{r}_i \eta_i^2 - \bar{g}\eta_1\eta_3 - \frac{1}{2}\sum_{i=1}^{3}(\nabla \eta_i)^2 + O(\eta_i^3) \ , \tag{2.16}$$

where

$$\bar{r}_1 = r_1 + 4(u+v)M_1^2 + 4uM_3^2 \ , \tag{2.17}$$

$$\bar{r}_2 = r_2 + (2u+v)M_3^2 + 4uM_1^2 + 2\sqrt{2}(2u-v)M_1 M_3 \ , \tag{2.18}$$

$$\bar{r}_3 = r_2 + 3(2u+v)M_3^2 + 4uM_1^2 - 2\sqrt{2}(2u-v)M_1 M_3 \ , \tag{2.19}$$

and

$$\bar{g} = 8uM_1 M_3 - \sqrt{2}(2u-v)M_3^2 \ . \tag{2.20}$$

The choice (2.14) and (2.15) for M_1 and M_3 ensures that no linear term in $\vec{\eta}$ enters into the Hamiltonian (2.16), and does not affect the calculations which follow. The quadratic term of the Hamiltonian (2.16) may be diagonalized by introducing new variables ψ_i, $i=1,2,3$ defined by

$$\psi_1 = \frac{1}{\sqrt{2}}(\bar{\eta}_3 + \eta_1) \ , \quad \psi_3 = \frac{1}{\sqrt{2}}(\bar{\eta}_3 - \eta_1) \ , \quad \psi_2 = \eta_2 \ , \tag{2.21}$$

with

$$\bar{\eta}_3 = \eta_3 \sqrt{\bar{r}_3/\bar{r}_1} \ . \tag{2.22}$$

The Hamiltonian (2.16) transforms into

$$\mathcal{H} = \mathcal{H}(M_1,M_3) - \frac{1}{2}\sum_{i=1}^{3} R_i \psi_i^2 - \frac{1}{2}\sum_{i=1}^{3}(\nabla \psi_i)^2 + O(\psi_i^3) \ , \tag{2.23}$$

where

$$R_1 = \bar{r}_1 - \bar{g}\sqrt{\bar{r}_1/\bar{r}_3} \ , \tag{2.24}$$

$$R_2 = \bar{r}_2 \ , \tag{2.25}$$

$$R_3 = \bar{r}_1 + \bar{g}\sqrt{\bar{r}_1/\bar{r}_3} \ . \tag{2.26}$$

The additional phase transition [line γ_2 in Fig. 3(b)] is associated with the component ψ_1. One then expects that in the vicinity of the transition $R_2, R_3 >> R_1$, which enables us to integrate ψ_2 and ψ_3 out of the problem using a perturbative expansion in powers of u and v. One then obtains an Ising-like effective Hamiltonian for the component ψ_1:

$$\mathcal{H}_{\rm eff} = -\tfrac{1}{2} r_{\rm eff}\psi_1^2 - \tfrac{1}{2}(\nabla \psi_1)^2 - w_{\rm eff}\psi_1^3 - u_{\rm eff}\psi_1^4 + O(\psi_1^5) \ , \tag{2.27}$$

where

$$r_{\rm eff} = R_1 + 0(u) = \bar{r}_1 - \bar{g}\sqrt{\bar{r}_1/\bar{r}_3} + O(u) \ , \tag{2.28}$$

and $w_{\rm eff}$ and $u_{\rm eff}$ are complicated functions of r_1, r_2, u, and v. Due to the presence of the cubic term in the Hamiltonian (2.27), any transition associated with it [i.e., line γ_2 in Fig. 3(b)] is expected to be first order. It is possible, however, that this transition will terminate at a liquid-gas-like critical point C, which is located at $r_{\rm eff}=w_{\rm eff}=0$.

First we prove the existence of the critical point C, to leading order, by showing that the requirement $r_{\rm eff}=w_{\rm eff}=0$ is satisfied automatically at the instability boundary $u=0$, for M_1 and M_3, which satisfy Eqs. (2.14) and (2.15). We then proceed to study the vicinity of the instability boundary $u \gtrsim 0$. Expanding in powers of u we find that to leading order

$$r_{\rm eff}=0+O(u) \ , \tag{2.29}$$

$$w_{\rm eff}=54\sqrt{2}uM_1+O(v^2M_1) \ , \tag{2.30}$$

$$u_{\rm eff}=-9u+O(v^2) \ . \tag{2.31}$$

These equations have a solution at $u=O(v^2)$. We have demonstrated the existence of the critical point only in the region $0<u<<v^2$. However, this result should hold throughout region (a) of Fig. 1, because the renormalization-group flows in this region drive u and v towards the instability boundary $u=0$. This ends the large-g limit calculations.

III. MEAN-FIELD ANALYSIS OF THE CUBIC MODEL WITH $w>0$

Mean-field theory always predicts a continuous phase transition for the Hamiltonian (1.1) if the quartic terms are positively definite, namely, when the Hamiltonian lies within the stability wedge. Therefore, to describe a first-order transition in the context of mean-field theory it is necessary to assume that the Hamiltonian lies outside the stability wedge and add a positive sixth-order term to stabilize the free energy. Consider the flow diagram associated with the $n=3$ cubic model (Fig. 1). If the initial physical parameters u and v lie in one of regions (1.3a) or (1.3b) [(a) and (b) in Fig. 1], the Hamiltonian flows, under renormalization-group transformations, to a region where it becomes thermodynamically unstable (either $u<0$, or $u+v<0$). It is therefore plausible that a mean-field analysis of the Hamiltonian in the unstable regions adding a positive sixth-order term will produce the same qualitative features as those obtained by perturbation expansion in regions (a) or (b) in Fig. 1 (see Refs. 15 and 16). We find indeed that this is the case and the resulting phase diagram is as predicted in Fig. 3(b). In particular no tricritical points are found on the critical lines α and β. Both lines terminate in critical end points (CE1 and CE2). We also find that the first-order line γ_2 terminates at a critical point C [see Fig. 3(b)]. As usual in mean-field calculations one neglects fluctuations and assumes a spatially homogeneous order parameter ϕ_1, ϕ_2, ϕ_3. As explained in Sec. II, it is possible to assume that ordering in the (ϕ_2, ϕ_3) subspace will involve only the component ϕ_3 due to the Potts symmetry of the term $\phi_3^3-3\phi_3\phi_2^2$. Thus, without loss of generality, we consider the Hamiltonian (2.5) with a sixth-order term but without the fluctuation terms. Setting $\phi_2=0$ yields a Landau Hamiltonian given by

$$\begin{aligned}\mathcal{H}_L=&\tfrac{1}{2}r_1\phi_1^2+\tfrac{1}{2}r_3\phi_3^2+\tfrac{1}{3}(u+v)\phi_1^4\\&+\tfrac{1}{4}(2u+v)\phi_3^4+2u\phi_1^2\phi_3^2\\&+\tilde{u}\phi_1\phi_3^3+u_6(\phi_1^2+\phi_3^2)^3 \ ,\end{aligned} \tag{3.1}$$

where

$$r_1=r-\tfrac{2}{3}g, \quad r_3=r+\tfrac{1}{3}g \ ,$$

$$\tilde{u}=-\frac{2\sqrt{2}}{3}(u-\tfrac{1}{2}v), \quad u_6>0 \ .$$

The order parameter associated with the critical line α is ϕ_1. At the critical line one has

$$\left(\frac{\partial^2\mathcal{H}_L}{\partial\phi_1^2}\right)_{\phi_1=\phi_3=0}=0 \ ,$$

which yields the equation

$$r_1=0 \ , \tag{3.2}$$

for the critical line α. The order parameter associated with the critical line β is ϕ_3. Notice, however, that as soon as ϕ_3 orders, it induces a secondary ordering of ϕ_1 via the term $\tilde{u}\phi_1\phi_3^3$ in (3.1). At the critical line one has

$$\left(\frac{\partial^2\mathcal{H}_L}{\partial\phi_3^2}\right)_{\phi_1=\phi_3=0}=0 \ ,$$

which yields the equation

$$r_2=0 \ , \tag{3.3}$$

for the critical line β. The choice $\phi_2=0$ ensures that $S_1=S_2$ [see Eq. (2.3)]. When $g=0$ the system orders along a cube axis $(v-2u>0)$, therefore one must have $S_1=S_2=0$ and $S_3\neq 0$. Inserting the last results in Eqs. (2.2) and (2.4) one obtains that on the line $g=0$

$$\phi_3=-\sqrt{2}\phi_1 \ . \tag{3.4}$$

To locate the first-order transition occurring at $g=0$ and to calculate the discontinuity in the order parameter at the transition, we use the necessary conditions for equilibrium given by $\partial\mathcal{H}_L/\partial\phi_1=0$, $\partial\mathcal{H}_L/\partial\phi_3=0$, and demand $\mathcal{H}_L(\phi_1,\phi_3)=0$ at the transition. These

three conditions together with Eq. (3.4) yield

$$r=\frac{u^2}{2u_6},\quad \phi_1^2=\frac{|u|}{6u_6}\ \text{with}\ \frac{\phi_3}{\phi_1}=-\sqrt{2}\ , \tag{3.5}$$

for the first-order transition occurring at $g=0$. The location of first-order lines, critical end points, and the critical point appearing in Figs. 3(b) and 3(a) involves a numerical analysis. With this in mind and also for computational convenience it is useful to define dimensionless variables and also to use ϕ_1 and ϕ_3/ϕ_1 as independent variables. We therefore define

$$(\phi_1,\phi_3)=\frac{|u|}{6u_6}(M_1,M_3)\ , \tag{3.6}$$

$$(r_1,r_2)=\frac{u^2}{2u_6}(R_1,R_2)\ , \tag{3.7}$$

$$M_3=x\sqrt{2}M_1\ , \tag{3.8}$$

$$c=(2u-v)/v\ . \tag{3.9}$$

Using these definitions we obtain

$$\mathcal{K}_L=\frac{|u|^3}{12u_6}\bar{\mathcal{K}}_L\ , \tag{3.10}$$

where

$$\bar{\mathcal{K}}_L=M_1^2\left[\frac{1}{2}(R_1+2x^2R_2)-\left[\frac{4(1+c/2)x^4-(8c/3)x^3+4(1+c)x^2+(1+c/3)}{3(1+c)}\right]M_1^2+\frac{1}{18}(1+2x^2)^3M_1^4\right]\ , \tag{3.11}$$

with $R_1=R-2G/3$ and $R_2=R+G/3$. Using the necessary conditions for equilibrium given by $\partial\bar{\mathcal{K}}_L/\partial M_3=\partial\bar{\mathcal{K}}_L/\partial M_1=0$, together with the definitions (3.6)–(3.9) one obtains M_1 as function of x

$$M_1^2=\frac{9}{4}\frac{(1+c)G}{c(2x^3-3x^2-3x+4)}\ . \tag{3.12}$$

The region of interest in the (u,v) plane ($u<0$) is such that $1+c<0$. The ratio $(1+c)/c$ is therefore positive. In the limit when $G\to 0$, the denominator goes to zero as well, yielding a finite M_1^2 which acquires the value 1 [see Eq. (3.5) together with the definition (3.6)]. The denominator has three real roots $x=-1$, $x=1/2$, and $x=2$. The value $x=-1$ corresponds to an ordering along a cube axis as given by Eq. (3.5). The value $x=2$ corresponds to an ordering along the cube diagonal $[11\bar{1}]$. This case will be studied in the next section. For $G<0$, we see that only those values of x for which the denominator is negative will yield a real solution for M_1. It is easy to see that this implies $x<-1$ (for the case of an easy axis along [001]) or $x>2$ (for the case of an easy axis along $[11\bar{1}]$). This observation simplifies enormously the numerical analysis and sets up an upper bound for x (for an easy axis along [001]) and a lower bound for x (for an easy axis along $[11\bar{1}]$). We can in principle insert (3.12) into (3.11) and obtain $\bar{\mathcal{K}}_L$ as function of x alone. To locate the critical point we demand

$$\frac{\partial\bar{\mathcal{K}}_L}{\partial x}=0,\quad \frac{\partial^2\bar{\mathcal{K}}_L}{\partial x^2}=0,\quad \frac{\partial^3\bar{\mathcal{K}}_L}{\partial x^3}=0\ ,$$

which yields three equations for the three unknowns x_c, R_c, and G_c. Inserting Eq. (3.12) into any one of the conditions for equilibrium it is possible to obtain a sixth-order polynomial for the variable x. To locate the first-order lines we proceed as follows. For a given value of G and R we calculate numerically the real roots of the polynomial and find the value of x for which $\bar{\mathcal{K}}_L$ is minimum. By scanning the (G,R) plane it is possible to obtain the first-order transition lines given in Fig. 3(b). We calculated numerically the discontinuity in the order parameter at the transition and found that it indeed decreases along γ_2, and finally vanishes at the critical point C. For $G<G_c$ ($G_c<0$), there is only one value of x which minimizes the free energy. Consider now the critical lines α and β. We will show that these lines terminate in the critical end points CE1 and CE2, respectively [see Fig. 3(b)]. The critical lines α and β are stable as long as $\bar{\mathcal{K}}_L>0$ for any $M_1\neq 0$ and x. At a critical end point $\bar{\mathcal{K}}_L$ satisfies $\bar{\mathcal{K}}_L(M_1,x)\geq 0$. However, there exists a solution ($M_1^E\neq 0$ and x_E) for which $\bar{\mathcal{K}}_L(M_1^E,x_E)=0$. This equation and the two minima conditions $\partial\bar{\mathcal{K}}_L/\partial M_1=0$, $\partial\bar{\mathcal{K}}_1/\partial x=0$, yield three equations for the four unknowns M_1^E, x_E, R_E, and G_E. The fourth equation is simply obtained by demanding that the critical end point is located on the critical line. Therefore to locate CE1 we demand $R_1=0$ and to locate CE2 we demand $R_2=0$. With the aid of these four conditions it is possible to obtain a polynominal equation for x_E which can be solved numerically. For CE1 we obtain

$$16cx_E^5-6(2+5c)x_E^4-16cx_E^3-4(3-c)x_E^2-(3+c)=0\ . \tag{3.13}$$

For CE2 we obtain

$$4(1+c/2)x_E^4+4x_E^2-4cx_E+(1+3c)=0\ . \tag{3.14}$$

Inserting the values of x_{E1} on x_{E2} obtained from (3.13) and (3.14) into (3.12) we obtain M_1^{E1} and

M_1^{E2}. By using any one of the conditions for equilibrium together with $R_1=0$, one obtains R_{E1},G_{E1}, and requiring $R_2=0$ one obtains R_{E2},G_{E2}. This ends the mean-field analysis. In this section we have demonstrated that the phase diagram associated with the Landau model (3.1) is indeed given by Fig. 3(b).

IV. CUBIC MODEL WITH $v<0$

A. Large anisotropy field analysis

In this section we analyze the cubic Hamiltonian (1.1) which lies in region (b) of Fig. 1 ($v<0$), namely, it is outside the domain of attraction of the isotropic fixed point, but within the stability wedge. To be specific $-u<v<0$ (see Fig. 1). From the arguments presented in the Introduction this Hamiltonian exhibits a first-order transition. Introducing the anisotropy field, g, given by (2.1) into the Hamiltonian and performing the coordinate transformation (2.2)–(2.4) we end up with the Hamiltonian (2.5). The gross features of the (r,g) phase diagram can be found quite easily. At $g=0$ and low temperatures the system orders along one of the cube diagonals [111], [11$\bar{1}$], [1$\bar{1}$1], [$\bar{1}$11]($v-2u<0$). The transition to this ordered phase is first order as explained in the Introduction. For large and positive g the components ϕ_2 and ϕ_3 are suppressed ($r_2 \gg r_1$) and the system will order in a phase characterized by $\langle\phi_1\rangle\neq 0$, $\langle\phi_2\rangle=\langle\phi_3\rangle=0$, namely, the order parameter will point along [111]. This phase transition is expected to be second order (Ising type with $u+v>0$). In this case there *is no competition* between the quadratic and quartic terms (both prefer an ordering along [111]). We therefore expect no additional transitions to occur in the ordered phase for $g>0$. Since for $g=0$ the transition from the disordered phase (PARA) to the ordered phase I is first order while for $g\gtrsim 1$ it is second order, we expect a tricritical point (TC) to occur. For large and negative g, ϕ_1 is suppressed ($r_1 \gg r_2$) and the system will order via a second-order xy-like transition (line β in Fig. 3a). Notice that immediately below the transition the component ϕ_1 will be induced via the term $(\phi_3^3-3\phi_3\phi_2^2)\phi_1$. The same arguments given in Sec. II apply here. In fact the phase diagram for $g<0$ is similar to the one studied in Secs. II and III [notice the similarity between the lower parts of Figs. 3(a) and 3(b)]. This is due to the fact that symmetry considerations are similar in both cases. By following the same arguments of Sec. II we expect an additional phase transition to occur inside phase II [line γ_2 of Fig. 3(a)], which, due to symmetry considerations, is expected to be first order and will terminate at a critical point C. A large negative g prefers an ordering in the (111) plane. As one lowers g the order parameter will leave the (111) plane and rotate towards the directions preferred by the quartic terms. From energy considerations it is clear that at $g=0$ it will align along one of the diagonals [11$\bar{1}$], [$\bar{1}$11], or [1$\bar{1}$1], but not along [111]. Therefore the line $g=0$ is expected to be a first-order line separating phase I (with $\vec{S}\parallel[111]$) from phase II which is an intermediate phase. Consider now the limit of large symmetry-breaking field $|g|\gtrsim 1$ ($g>0$), and $u,v \ll 1$. Furthermore, assume that the Hamiltonian, although stable, is very close to the instability limit, namely, $0<u+v \ll O(u,v)$. In this case $r_2=O(1)$, and the components ϕ_2 and ϕ_3 can be integrated out using a perturbation expansion in powers of u and v. One then obtains the same reduced Hamiltonian given in Eq. (2.6) with (2.7)–(2.9).

The main difference between the present analysis and the one presented in Sec. II is that in this case we shall be able to obtain a tricritical point. In three or more dimensions the reduced Hamiltonian (2.6) will yield a continuous transition for $r_1=O(u,v)$ and $u_{\rm eff}\gtrsim 0$, a first-order transition for $u_{\rm eff}\lesssim 0 (u_6>0)$, and a tricritical point at $r_{\rm eff}=r_t\simeq O(u_6)=O(u^3,v^3)$, and $u_{\rm eff}=u_t=O(u_6)=O(u^3,v^3)$. The tricritical point can therefore be located to leading order in u and v by solving the equations

$$r_t(r,g,u,v)=u_t(r,g,u,v)=0 \ . \tag{4.1}$$

Consider the integral $A_2(r_2,d)$: this is a decreasing function of r_2 which approaches zero as $r_2\to\infty$. Let us fix u and v and vary r_2. For large enough $r_2=r+g/3$, namely, for large enough g, one has $u_{\rm eff}\simeq(u+v)/3>0$, and the Hamiltonian (2.6) exhibits a continuous transition occurring at the line α given by $r_1=O(u,v)$, [see Fig. 3(a)]. As r_2 is decreased, however, the integral $A_2(r_2,d)$ becomes large and $u_{\rm eff}$ will change sign. For smaller r_2 the transition thus becomes first order. The system exhibits a tricritical point at $r_2=r_{2t}$ given by

$$A_2(r_{2t},d)=\frac{1}{24}\frac{u+v}{u^2} \ . \tag{4.2}$$

Note that our approximation is valid only if $r_{2t}\gtrsim 1$ [with $A_2(r_{2t},d)\lesssim O(1)$], hence the existence of the tricritical point has been demonstrated only in the region $0<u+v\lesssim u^2$. However, one should notice that provided one starts out in region (b) of Fig. 1, the Hamiltonian (2.6) will flow, under renormalization-group transformation, towards the instability limit $u+v=0$. We therefore expect our results to hold in the entire region (b). The large anisotropy limit analysis for the case $|g|\gtrsim 1$ and $g<0$, follows exactly as in Sec. II. One therefore expects a critical line β given by $r_2=O(u,v)$ separating the disordered phase (PARA) from phase II. This critical line terminates in a critical end point CE [see Fig. 3(a)]. The critical point C is located as in Sec. II. This ends the large-g limit analysis.

B. Mean-field analysis

As explained in Sec. III in order to describe a first-order transition in the context of mean-field theory it is necessary to assume that the Hamiltonian lies outside the stability wedge and add a positive sixth-order term to stabilize the free energy. Following the argument of Sec. III it is plausible to assume that a mean-field analysis of the Hamiltonian (2.5) in the unstable region $u+v<0$, adding a sixth-order term, will produce the same qualitative features as those obtained by perturbation expansion in region (b) of Fig. 2 ($-u<v<0$). We find that indeed this is the case and the resulting phase diagram is as predicted in Fig. 3(a). In particular no tricritical point is found on the critical line β, which terminates in a critical end point CE [see Fig. 3(a)]. We also find that the first-order line γ_2 terminates at a critical point C [see Fig. 3(a)]. We have stressed the fact that within the stability region (b) in the (u,v) plane, classical Landau (or mean-field) theory can give a qualitatively misleading phase diagram insofar as no tricritical points and associated first-order lines are predicted. However, within a broader parameter space in which a positive sixth-order term is included in the Hamiltonian, the theory is less misleading. Then the instability condition $v\leq 0$ needed for tricriticality is replaced by the requirement $u+v<0$. The sixth-order term ensures stability of the free energy, and a line of tricritical points occurs when $u+v=0$ (where the quartic terms become unstable[12]). By following the arguments of Sec. III we analyze the Hamiltonian (3.1) in the region $v+u<0$. The order parameter associated with the critical line β is ϕ_3. Notice that as soon as ϕ_3 orders it induces a secondary ordering of ϕ_1 via the term $\tilde{u}\phi_1\phi_3^3$ in (3.1). At the critical line one has

$$\left[\frac{\partial^2 \mathcal{K}_L}{\partial \phi_3^2}\right]_{\phi_1=\phi_3=0}=0 \ ,$$

which yields the equation

$$r_2=0 \ , \tag{4.3}$$

for the critical line β. For a very large and negative g the system orders in the (111) plane. As one lowers g in the ordered phase the order parameter rotates away from the (111) plane and from energy considerations one can show that as g approaches zero from below, the order parameter will align itself along $[11\bar{1}]$ or $[\bar{1}11]$ or $[1\bar{1}1]$ but not along [111]. Taking also into account that the components of $\vec{S}$ satisfy $S_1=S_2$ [for our choice $\phi_2=0$, see Eq. (2.3)], one finds the following relation between ϕ_3 and ϕ_1 as g approaches zero from below

$$\phi_3=2\sqrt{2}\phi_1 \ . \tag{4.4}$$

To locate the first-order transition occurring at $g=0$, and to calculate the discontinuity in the order parameter at the transition, we use the necessary conditions for equilibrium given by $\partial \mathcal{K}_L/\partial\phi_1=0$, $\partial \mathcal{K}_L/\partial\phi_3=0$, and demand $\mathcal{K}_L(\phi_1,\phi_3)=0$ at the transition [coexistence with the disordered phase $\phi_1=\phi_2=0$, for which $\mathcal{K}_L(0)=0$]. These three conditions together with Eq. (4.4) yield

$$r=\frac{(u+v)^2}{18u_6}; \quad \phi_1^2=\frac{|u+v|}{54u_6} \quad \text{with} \quad \frac{\phi_3}{\phi_1}=2\sqrt{2} \ , \tag{4.5}$$

at the first-order transition occurring for $g=0$.

As explained above, for $g>0$ there is no competition between the quadratic and the quartic terms, therefore the system will order along [111]. The order parameter describing this phase transition is therefore ϕ_1. Setting $\phi_3=0$ in Eq. (3.1) one obtains

$$\mathcal{K}_L=\tfrac{1}{2}r_1\phi_1^2+\tfrac{1}{3}(u+v)\phi_1^4+u_6\phi_1^6+O(\phi_1^8) \ , \tag{4.6}$$

with $r_1=r-2g/3$, $u+v<0$, and $u_6>0$.

The Hamiltonian (4.6) yields a first-order transition as long as $u+v<0$, $u_6>0$. Therefore, the tricritical point TC of Fig. 3(a) cannot be obtained within mean-field theory in the (r,g) plane. Only in the broader parameter space (r,g,u,v) can we obtain a line of tricritical points at the plane $u+v=0$. To locate the first-order transition line separating the disordered phase (PARA) from phase I we demand $\partial \mathcal{K}_L/\partial\phi_1=0$ and $H_L(\phi_1)=0$. This yields

$$r_1=\frac{(u+v)^2}{18u_6}, \quad \phi_1^2=\frac{|u+v|}{6u_6}, \quad \phi_3=0 \ , \tag{4.7}$$

at the first-order transition occurring for $g>0$. The phase diagram for $g<0$ is calculated numerically following exactly the same steps outlined in Sec. III. The same qualitative results are obtained. This is due to the fact that for $g<0$ both problems have the same symmetry. This ends the mean-field analysis. In this section we have demonstrated that the phase diagram associated with the Landau model (3.1) is in qualitative agreement with that in Fig. 3(a).

V. RENORMALIZATION-GROUP ANALYSIS

A. Scaling arguments

In this section we study the occurrence of critical end points at small anisotropy field $|g|\ll 1$, for $w\gtrsim 0$. Using scaling arguments[25] we define a universal amplitude ratio associated with the two critical end points CE1 and CE2, induced by the symmetry-breaking field [Fig. 3(b)]. This universal amplitude ratio is then calculated to leading (zeroth) order in ϵ using renormalization-group integral methods.[16,26,27]

Consider the flow diagram of Fig. 1. As explained

above the line $w=v-3u=0$ is the borderline of tricriticality [Eq. (1.3a)]. For $g=0$ and $w<0$, the isotropic fixed point is both accessible and stable and therefore the transition is continuous, while for $g=0$ and $w>0$ the transition is first order. One can therefore apply scaling arguments to discuss the phase diagram in the vicinity of the $g=w=0$ (cubic) fixed point which has the character of a multicritical point. According to general scaling theory,[25] the singular part of the free energy derived from the Hamiltonian (2.5) should vary as

$$F(t,g,w) \approx t^{1-\alpha_w} \tilde{F}(g/t^{\phi_g}, w/t^{\phi_w}) \ , \tag{5.1}$$

in the limit $t \to 0$, $g \to 0$ and $w \to 0$. As usual $t=1-T/T_c$, where T_c is the critical temperature for $g=w=0$, α_w is the critical exponent for the specific heat and ϕ_g and ϕ_w are the appropriate crossover exponents with respect to the cubic fixed point.[21] The existence of a multicritical point (M) is necessarily associated with singular behavior of the scaling function $\tilde{F}(x,y)$ at some point (x_M, y_M).

This singularity will, in fact, describe a line of multicritical points in the (t,g,w) space. We expect two lines of critical end points: one for $g>0$ and one for $g<0$. In the scaling limit (5.1) the projection of the lines of critical end points on the (g,t) plane must take the form [see Fig. 3(b)]

$$g = A_{\mathrm{CE1}} t^{\phi_g} \quad \text{for } g>0 \ , \tag{5.2}$$

and

$$g = -A_{\mathrm{CE2}} t^{\phi_g} \quad \text{for } g<0 \ . \tag{5.3}$$

The ratio $A_{\mathrm{CE2}}/A_{\mathrm{CE2}}$ should be a universal quantity independent of the irrelevant variables and equal to $x_{\mathrm{CE1}}/x_{\mathrm{CE2}}$. This ratio is calculated to leading (zeroth) order in $\epsilon=4-d$ using techniques developed in Refs. 12 and 16.

B. Recursion relations

As explained above, the integration over the component ϕ_1 is justified only when $r_1=O(1)$ ($|g| \gtrsim 1$, $g<0$) and the integration over the components ϕ_2 and ϕ_3 is justified only when $r_2=0(1)$ ($|g| \gtrsim 1$, $g>0$). However, for small negative g in the critical region $r_2=r-O(g) \simeq 0$, we also have $r_1=r+O(g)$ small; and for small positive g in the critical region $r_1=r-O(g) \simeq 0$ we also have $r_2=r+O(g)$ small. The way to treat this situation is to use the renormalization-group trajectory integral method of Rudnick and Nelson,[26] to relate the initial Hamiltonian with small r and g to a renormalized Hamiltonian in which $r_1=O(1)$ or $r_2=O(1)$. Only then is the ϕ_1 component [for $r_1=O(1)$] or the ϕ_2 and ϕ_3 components [for $r_2=O(1)$] integrated out, and the analysis developed in Secs. II and IV can be applied. The answers obtained in terms of the renormalized parameters u', v', r', g' are then related to the initial parameters u, v, r, g by solving the recursion relations of the renormalization-group transformation.[26,27]

Consider the Hamiltonian (2.5). Under action of the renormalization group[20] it is transformed, but to leading order $\epsilon=4-d$, the renormalized Hamiltonians $\mathcal{H}(l)$ remain in the parameter space r_1, r_2, u, v. To this order the differential recursion relations for $r_1(l), r_2(l), u(l)$ and $v(l)$ are found to be

$$\frac{dr_1}{dl} = 2r_1 + 4K_4(u+v)(1-r_1) + 8K_4 u(1-r_2) \ , \tag{5.4}$$

$$\frac{dr_2}{dl} = 2r_2 + 4K_4(2u+v)(1-r_2) + 4K_4 u(1-r_1) \ , \tag{5.5}$$

$$\frac{du}{dl} = \epsilon u - 36K_4 u^2 - 2K_4 v^2 \ , \tag{5.6}$$

$$\frac{dv}{dl} = \epsilon v - 10K_4 v^2 - 24K_4 uv \ , \tag{5.7}$$

where $K_4 = \frac{1}{8}\pi^2$. Our procedure will be as follows. Equations (5.4)–(5.7) will be solved in an approximation valid for any l for which $r_1(l) \lesssim O(1)$ (if initially $r_1 > r_2$) or for which $r_2(l) \lesssim O(1)$ (if initially $r_2 > r_1$). We will then select a value of l^* by requiring $r_1(l^*)=1+O(\epsilon)$ or $r_2(l^*)=1+O(\epsilon)$, respectively. At this point the renormalized Hamiltonian $\mathcal{H}(l^*)$ is noncritical with respect to fluctuations of that order parameter component whose r value is unity. Thus, the trace over the noncritical component can be performed, keeping terms of appropriate order. After this step one obtains a reduced Hamiltonian (which depends only on the remaining variables) whose critical behavior we analyze as in Secs. III and IV. The coupled (u,v) differential Eqs. (5.6) and (5.7) have been solved by Rudnick.[9] For the present analysis we will not need the explicit solutions, rather we shall use the fact that $u(l)$ and $v(l)$ remain of order u^* and v^*, that is, of order ϵ (u^* and v^* being the fixed point values about which the analysis is performed). In order to solve Eqs. (5.4) and (5.5) we reintroduce the original variables $g=r_2-r_1$ and $r=r_1/3+2r_2/3$ in terms of which the recursion relations decouple to $O(\epsilon)$. It proves convenient to express these decoupled equations in terms of

$$\Delta u(l) = u(l) - u^*, \quad \Delta v(l) = v(l) - v^* \ . \tag{5.8}$$

Using these definitions, the equations for g and r become

$$\frac{dg}{dl} = \lambda_2 g - 4K_4 \Delta v g \ , \tag{5.9}$$

$$\frac{dr}{dl} = \lambda_1 r + 4K_4(3u^*+v^*) + 4K_4(3\Delta u + \Delta v)(1-r) \ , \tag{5.10}$$

where the eigenvalues

$$\lambda_1 = 2 - 4K_4(3u^* + v^*), \quad \lambda_2 = 2 - 4K_4 v^* \ , \tag{5.11}$$

correspond to the unstable, cubic fixed point. Given $u(l)$ and $v(l)$ the solutions of (5.9) and (5.10) may be written

$$g(l) = e^{\lambda_2 l}\bar{g}(l) \ , \tag{5.12}$$

$$\bar{g}(l) = g_0 \exp\left[-\int_0^l [4K_4 \Delta v(l')]\, dl'\right] \ , \tag{5.13}$$

and

$$r(l) = t(l) - 6K_4 u(l) - 2K_4 v(l) \ ,$$

$$t(l) = e^{\lambda_1 l}\bar{t}(l) \ , \tag{5.14}$$

$$\bar{t}(l) = t_0 \exp\left[-\int_0^l [12K_4 \Delta u(l') + 4K_4 \Delta v(l')]\, dl'\right] \ . \tag{5.15}$$

Having solved the recursion relations we turn now to locate the critical end points and to determine the universal amplitude ratio defined before.

C. Location of critical end points in the region $w > 0$

If initially $w \gtrsim 0$, then the system is in the close vicinity of the unstable cubic fixed point for which

$$u^* = \frac{\epsilon}{54K_4}, \quad v^* = \frac{\epsilon}{18K_4} \ ,$$

$$\lambda_1 = 2 - \tfrac{4}{9}\epsilon, \quad \lambda_2 = 2 - \tfrac{2}{9}\epsilon \ . \tag{5.16}$$

Under the renormalization-group transformation, u and v will therefore flow away from the fixed point towards the instability limit $u = 0$. Recall that to leading order this flow is not influenced by the quadratic symmetry-breaking perturbation. Assume now that initially $r_2 \gtrsim r_1 (g \gtrsim 0)$. In this case we have to iterate the recursion relations up to a value l_1^* for which

$$r_2(l_1^*) = 1 + O(\epsilon) \ . \tag{5.17}$$

Three possible cases may occur. (a) The flow in the (u, v) plane does not reach the instability limit, namely, $u(l_1^*)$ is still positive. (b) The flow in the (u, v) plane crosses the instability limit, namely $u(l_1^*) < 0$. (c) The flow in the (u, v) plane reaches precisely to the instability limit, namely $u(l_1^*) = 0$. In case (a) the renormalized Hamiltonian $\mathcal{H}(l_1^*)$ is stable and we can integrate out the noncritical variables ϕ_2 and ϕ_3 to obtain a reduced Ising-like Hamiltonian given in (2.6), where now r_{eff} and u_{eff} [see Eqs. (2.7) and (2.8)] are functions of l_1^*. In $\mathcal{H}_{\text{eff}}(l_1^*)$ we easily identify a temperaturelike variable $t_{\text{eff}}(l_1^*) = r_1(l_1^*) + O(\epsilon)$. In this case $u_{\text{eff}}(l_1^*)$ is always positive [see (2.8)], thus $t_{\text{eff}}(l_1^*) = 0$ defines a critical (reduced) Hamiltonian. In case (b) the renormalized Hamiltonian $\mathcal{H}(l_1^*)$ contains an instability in the (ϕ_2, ϕ_3) subspace, and one has to modify the renormalization-group transformation.[9] In case (c) the instability in the (ϕ_2, ϕ_3) subspace is about to occur. Therefore the components ϕ_2 and ϕ_3 can still be integrated out to obtain the reduced Hamiltonian of case (a). In this case, however,

$$t_{\text{eff}}(l_1)^* = r_1(l_1^*) + O(\epsilon) = 0 \ , \tag{5.18}$$

together with

$$u(l_1^*) = 0 \ , \tag{5.19}$$

define a critical end point for $g > 0$.[16] The same argument applies when initially $r_1 \gtrsim r_2 (g \lesssim 0)$. In this case we iterate up to a value l_2^* for which

$$r_1(l_2^*) = 1 + O(\epsilon) \ . \tag{5.20}$$

If $u(l_2^*) > 0$ then we can integrate the variable ϕ_1 to obtain a reduced xy-like Hamiltonian given in (2.10) where now r_{eff} and u_{eff} [see Eqs. (2.11) and (2.12)] are functions of l_2^*. Identifying a temperaturelike variable $t_{\text{eff}}(l_2^*) = r_2(l_2^*) + O(\epsilon)$ and demanding

$$t_{\text{eff}}(l_2^*) = r_2(l_2^*) + O(\epsilon) = 0 \ , \tag{5.21}$$

together with

$$u(l_2^*) = 0 \ , \tag{5.22}$$

defines a critical end point for $g < 0$. Equations (5.19) and (5.22) indicate that we iterate up to a value $l = L$ at which the instability line $u = 0$ is reached, therefore to leading order $l_1^* = l_2^* = L$. This point, first noticed by Kerszberg and Mukamel,[16] simplifies the forthcoming calculations. To locate the critical end point (CE1) for $g > 0$ we have to solve Eqs. (5.17), (5.18), and (5.19), which impose three conditions on the five variables t_0, g_0, u_0, v_0, and l_1^*. Thus, for fixed u_0 and v_0 we can, in principle, eliminate l_1^* and obtain $(t_0, g_0)_{\text{CE1}}$. Following Ref. 12 we define

$$z = \frac{\bar{g}(l_1^*)}{[\bar{t}(l_1^*)]^{\phi_g}}, \quad \text{with } \phi_g = \frac{\lambda_2}{\lambda_1} \ , \tag{5.23}$$

and

$$e^{l_1^*} = [\bar{t}(l_1^*)]^{-1/\lambda_1}\psi \ , \tag{5.24}$$

with $\bar{g}(l)$ and $\bar{t}(l)$ given in Eqs. (5.13) and (5.15). Substituting in (5.17) we obtain

$$\psi^{\lambda_1} + \tfrac{1}{3} z \psi^{\lambda_2} = 1 \ , \tag{5.25}$$

from which we see that ψ is a function of z alone. The criticality condition (5.18) now becomes

$$\psi^{\lambda_1} - \tfrac{2}{3} z \psi^{\lambda_2} = 0 \ , \tag{5.26}$$

which on using (5.25) and (5.16) for λ_1 and λ_2, yields

$$z=\frac{3}{2} \ , \tag{5.27}$$

to leading order in ϵ.[12,16] Finally we invoke the condition (5.19) to obtain a critical end point. This means that for a given u_0 and v_0 we must also have $l_1^*=L$ where L is the value of l for which the flow in the (u,v) plane (which, one recalls, is decoupled to leading order) goes from u_0, v_0 to $u(L), v(L)$ such that the condition (5.19) is satisfied. Combining this requirement with (5.27) and (5.23) yields

$$\bar{g}(L)/[\bar{t}(L)]^{\phi_g}=\frac{3}{2} \ , \tag{5.28}$$

with

$$g_0=g_{\mathrm{CE1}}, \quad t_0=t_{\mathrm{CE1}} \ , \tag{5.29}$$

where g_{CE1} and t_{CE1} denote the critical end point values in the initial Hamiltonian. Using the definitions (5.13) and (5.15) yields

$$g_{\mathrm{CE1}}=A_{\mathrm{CE1}}t_{\mathrm{CE1}}^{\phi_g} \ , \tag{5.30}$$

$$A_{\mathrm{CE1}}=\frac{3}{2}\exp\left[-\int_0^L 12K_4\Delta u(l')\,dl'\right] \ . \tag{5.31}$$

For the case $g<0$, Eqs. (5.25) and (5.26) are interchanged (therefore $z=3$) [see Eqs. (5.20) and (5.21)]. As explained before, the condition (5.22) implies that $l_2^*=L$. Carrying out the same analysis as before one obtains

$$g_{\mathrm{CE2}}=-A_{\mathrm{CE2}}t_{\mathrm{CE2}}^{\phi_g} \ , \tag{5.32}$$

where

$$A_{\mathrm{CE2}}=3\exp\left[-\int_0^L 12K_4\Delta u(l')\,dl'\right] \ . \tag{5.33}$$

The amplitude ratio is given by

$$A_{\mathrm{CE1}}/A_{\mathrm{CE2}}=\frac{1}{2} \ . \tag{5.34}$$

This result is subject to corrections of order ϵ.

The crucial point in this calculation is that $l_1^*=l_2^*=L$ and therefore the integrals in (5.31) and (5.33) cancel. This will always be the case if one requires the flow in the (u,v) plane must terminate at a certain line.

VI. CONCLUSIONS

In this paper we have studied the effects of an off-diagonal quadratic perturbation, g, on a three-component cubic model with no accessible fixed point. We have shown that this perturbation is capable of inducing a crossover from first order to continuous transition which results in complicated (g,T) phase diagrams [see Figs. 3(a) and 3(b)]. The (g,T) phase diagrams exhibit critical, tricritical, and critical end points. Our results are based on large-g expansion, mean-field analysis and renormalization-group techniques. We suggest that the crossover found in this work may be observed in certain $n=3$ cubic crystals which undergo a structual phase transition. The compounds $RbCaF_3$,[19(c)] $KMnF_3$,[28] and $BaTiO_3$ (Ref. 29) are cubic crystals which undergo a first-order cubic to tetragonal $(v-2u>0)$ displacive phase transition. We suggest that the application of a uniaxial stress along [111] may generate the phase diagram given in Fig. 3(b). Note, however, that the dispersion relation in $RbCaF_3$ and $KMnF_3$ is strongly anisotropic,[19] suggesting that a crossover to Lifshitz type behavior[30] should occur in this systems.[31] Again, this may complicate the phase diagrams. We hope to study this problem in a future work.

ACKNOWLEDGMENTS

We thank M. Kerszberg for helpful comments. One of the authors D.B. would like to thank Professor A. Aharony, his research advisor, for fruitful conversations and instructive comments. This work was supported in part by a grant from the U.S.-Israel Binational Science Foundation (BSF), Jerusalem, Israel.

*On leave from the Weizmann Institute of Sciences, Rehovot, Israel.

[1]D. Mukamel and S. Krinsky, Phys. Rev. B 13, 5065, 5078 (1976); P. Bak and D. Mukamel, *ibid.* 13, 5086 (1976).

[2]P. Bak, S. Krinsky, and D. Mukamel, Phys. Rev. Lett. 36, 52 (1976).

[3]S. A. Brazovskii and I. E. Dzyaloshinskii, Pis'ma Zh. Eksp. Teor. Fiz. 21, 360 (1975) [JETP Lett. 21, 164 (1975)].

[4]I. E. Dzyaloshinskii, Zh. Eksp. Teor. Fiz. 72, 1930 (1977) [Sov. Phys. JETP 45, 1014 (1977)].

[5]V. A. Alessandrini, A. P. Cracknell, and J. A. Przystawa, Commun. Phys. 1, 51 (1976).

[6]D. Mukamel and D. J. Wallace, J. Phys. C 13, L851 (1979).

[7]O. G. Mouritsen, S. J. Knak Jensen, and P. Bak, Phys. Rev. Lett. 39, 629 (1977).

[8]T. Nattermann and S. Trimper, J. Phys. A 8, 2000 (1975); T. Nattermann, J. Phys. C 9, 3337 (1976).

[9]J. Rudnick, Phys. Rev. B 18, 1406 (1978).

[10]I. F. Lyuksyutov and V. Pokrovskii, Pis'ma Zh. Tekh. Fiz. 21, 22 (1975) [JETP Lett. 21, 9 (1975)].

[11]P. Bak, S. Krinsky, and D. Mukamel, Phys. Rev. Lett. 36, 829 (1976).

[12]E. Domany, D. Mukamel, and M. E. Fisher, Phys. Rev. B 15, 5432 (1977).

[13]J. Sólyom and G. S. Grest, Phys. Rev. B 16, 2235 (1977).
[14]S. J. Knak Jensen, O. G. Mouritsen, E. K. Hansen, and P. Bak, Phys. Rev. B 19, 5886 (1979).
[15]M. Kerszberg and D. Mukamel, Phys. Rev. Lett. 43, 293 (1979).
[16]M. Kerszberg and D. Mukamel, Phys. Rev. B 23, 3943, 3953 (1981).
[17]D. Bloch, C. Vettier, and P. Burlet, Phys. Lett. 75A, 301 (1980).
[18]D. Bloch, D. Hermann-Ronzaud, C. Vettier, W. B. Yelon, and R. Alben, Phys. Rev. Lett. 35, 963 (1975).
[19](a) J. Y. Buzarè, J. C. Fayet, W. Berlinger, and K. A. Müller, Phys. Rev. Lett. 42, 465 (1979); (b) K. A. Müller, W. Berlinger, J. Y. Buzaré, and J. C. Fayet, Phys. Rev. B 21, 1763 (1980); (c) A. Aharony and A. D. Bruce, Phys. Rev. Lett. 42, 462 (1979), and references therein.
[20]See, e.g., (a) K. G. Wilson and J. B. Kogut, Phys. Rep. 12C, 75 (1974); (b) *Phase Transitions and Critical Phenomena,* edited by C. Domb and M. S. Green (Academic, New York, 1976).
[21]For a discussion of the renormalization-group flows of the cubic model, see, e.g., A. Aharony in Ref. 20(b).
[22]A. D. Bruce and A. Aharony, Phys. Rev. B 11, 478 (1975); K. A. Müller, W. Berlinger, and J. C. Slonczewski, Phys. Rev. Lett. 25, 734 (1970).
[23]A. Aharony, K. A. Müller, and W. Berlinger, Phys. Rev. Lett. 38, 33 (1977); J. Rudnick, J. Phys. A 8, 1125 (1975).
[24]D. Mukamel, M. E. Fisher, and E. Domany, Phys. Rev. Lett. 37, 565 (1976).
[25]See, e.g., M. E. Fisher, in *Proceedings of the Twenty-Fourth Nobel Symposium on Collective Properties of Physical Systems, Aspenaasgarden, Sweden, 1973,* edited by B. Lundgvist and S. Lundgvist (Nobel Foundation, Stockholm, 1973), Vol. 24, p. 16; P. Pfeuty, D. Jasnow, and M. E. Fisher, Phys. Rev. B 10, 2088 (1974).
[26]J. Rudnick and D. R. Nelson, Phys. Rev. B 13, 2208 (1976).
[27]D. R. Nelson and E. Domany, Phys. Rev. 13, 236 (1976); E. Domany, D. R. Nelson, and M. E. Fisher, Phys. Rev. B 15, 3453 (1977); E. Domany and M. E. Fisher, Phys. Rev. B 15, 3510 (1977).
[28]G. Shirane, V. J. Minkiewicz, and A. Linz, Solid State Commun. 8, 1941 (1970).
[29]See, e.g., Y. G. Yamada, A. Shirane, and A. Linz, Phys. Rev. 177, 848 (1969); G. Samara, Ferroelectrics 2, 277 (1971); R. Clarke and L. Benguigui, J. Phys. C 10, 1963 (1977).
[30]R. M. Hornreich, M. Luban, and S. Shtrikman, Phys. Rev. Lett. 35, 1678 (1975).
[31]This type of crossover was predicted by Aharony and Bruce for a uniaxial stress along the [100] axis, and was recently observed experimentally (see Ref. 19).